자원환경지질, 제35권, 제3호, 211-220, 2002
Econ. Environ. Geol., 35(3), 211-220, 2002

Alteration and Mineralization in the Xiaoxinancha Porphyry Copper Deposit, Yianbin, China: Fluid Inclusion and Sulfur Isotope Study

Chil-Sup So[1], Bai-Lu Jin[2], Seong-Taek Yun[1]*, Chul-Ho Heo[1], Seung-Jun Youm[1]

[1]Department of Earth and Environmental Sciences, Korea University, Seoul 136-701, Korea(고려대학교 지구환경과학과)
[2]Geological Survey #6, Bureau of Geology and Mineral Resources of Jilin Province, China

중국 연변 쇼시난차 반암동 광상의 광화작용 및 변질작용: 유체포유물 및 황 동위원소 연구

소칠섭[1] · Bai-Lu Jin[2] · 윤성택[1]* · 허철호[1] · 염승준[1]

[1]Department of Earth and Environmental Sciences, Korea University, Seoul 136-701, Korea(고려대학교 지구환경과학과)
[2]중국 길림성 지광국 제 6 지질조사소

중국 북경에서 북북동쪽으로 800 km에 위치한 길림성의 쇼시난차 동-금 광상은 섬록암에 배태되어 있다. 쇼시난차 동-금 광상의 광석은 망상세맥상으로 산출되며, potassic 및 phyllic변질대에 농집되어 있다. 쇼시난차 동-금 광상의 남측 및 북측광체의 품위는 각각 0.8% Cu, 3.64 g/t Au 및 0.63% Cu, 3.80 g/t Au이다. 본 광상의 열수변질 작용은 암주에 집중되어 있고, 암주의 정치와 폭넓게 관련되어있는 것으로 사료된다. 초기 열수변질 작용은 K-변질작용이 지배적이며, 시간이 지나면서 프로필라이트화 작용으로 전환되는 양상을 보인다. 본 광상에서는 적철석과 수반된 휘동석이 채광품위의 동을 산출하고 있으며, 황동석, 반동석, 석영, 녹염석, 녹니석 및 방해석의 광물조합이 전형적으로 관찰된다. 상기 광물조합외에 본 연구에서 인지된 기타 광물들에는 황철석, 백철석, 자연금, 에렉트럼, hessite, hedleyite, volynskite, galenobismutite, covellite 및 goethite등이 있다. 유체포유물 자료에 의하면, 본 동-금 광상은 시간이 지나면서 희석되고 차가운 천수의 혼입에 의한 냉각작용의 결과로 형성되었음을 지시하고 있다. 광화시기별로 보면, 광화 2기 초기에는 약 497°C에서 비등현상이 발생하고 시간이 지나면서 균질화 온도가 100°C정도 낮은 암염을 배태하고 있는 제 3형 유체포유물이 포획된다. 그리고, 광화 2기 맥내 제 3형 유체포유물의 염농도는 383°~495°C의 균질화 온도에서 54.3~66.9 wt.%의 상당염농도에 해당되며, 1 km이하의 생성심도를 지시하고 있다. 광화 3기맥의 제 1형의 함동 유체는 168°~365°C의 균질화온도와 1.1~9.0 wt.% 상당 염농도를 보이며, 해당 유체포유물들은 심하게 균열된 각력암을 배태하고 있는 석영맥내에 포획되어 있다. 이는 비등증거를 강하게 지시하고 있으며, 50~80 bar의 정수압에 해당된다. 본 광상의 황화물의 $\delta^{34}S$값은 후기로 가면서 미약하게 증가하는 경향을 보이며, 계산된 $\delta^{34}S_{H2S}$값은 0.8~3.7‰에 해당한다. 산소분압이 감소했으리라는 광물학적 증거는 없으며, 광화유체의 산소분압은 자철석과의 반응을 통해서 완충되었으리라 사료된다. 이와같은 사실을 종합해 본 결과, 황화물의 $\delta^{34}S_{H2S}$값은 쇼시난차 동-금 광상의 함동금 열수유체에 두 가지 정도의 황source가 병합되었으리라 추정할 수 있다. 첫번째 source는 동위원소적으로 가벼운 1~2‰의 $\delta^{34}S$값을 지닌 광화작용과 관련된 중생대 화강암이다. 이는 본 광상지역의 모암으로서의 섬록암이 plagiogranite를 관입하고 있다는 사실로부터 추론 가능하다. 그리고, 두번째 source는 > 4.0‰의 $\delta^{34}S$값을 지닌 동위원소적으로 더욱 무거운 source로서, 산출이 미약하여 지질도상에는 기재되어 있지 않지만 국부적인 반암의 존재를 상정할 수 있다.

주요어 : 변질작용, 광화작용, 반암동, 유체포유물, 황동위원소

The Xiaoxinancha Cu-Au deposit in the Jilin province, located in NNE 800 km of Beijing, is hosted by diorite. The ore mineralization of Xiaoxinancha Cu-Au deposit show a stockwork occurrence that is concentrated on the potassic and phyllic alteration zones. The Xiaoxinancha Cu-Au deposit in the south is being mined with its reserves grading 0.8% Cu, 3.64 g/t Au and 16.8 g/t Ag and in the north, grading 0.63% Cu, 3.80 g/t Au and 6.8 g/t Ag. The alteration assemblage occurs as a supergene blanket over deposit. Hydrothermal alteration at the Xiaoxinancha Cu-Au deposit is centered about the stock and was extensively related to the emplacement of the stock. Early hydrothermal alteration was dominantly

*Corresponding author: styun@mail.korea.ac.kr

potassic and followed by propylitic alteration. Chalcocite, often associated with hematite, account for the ore-grade copper, while chalcopyrite, bornite, quartz, epidote, chlorite and calcite constitute the typical gangue assemblage. Other minor opaque phases include pyrite, marcasite, native gold, electrum, hessite, hedleyite, volynskite, galenobismutite, covellite and goethite. Fluid inclusion data indicate that the formation of this porphyry copper deposit is thought to be a result of cooling followed by mixing with dilute and cooler meteoric water with time. In stage II vein, early boiling occurred at 497°C was succeeded by the occurrence of halite-bearing type III fluid inclusion with homogenization temperature as much as 100°C lower. The salinities of type III fluid inclusion in stage II vein are 54.3 to 66.9 wt.% NaCl + KCl equiv. at 383° to 495°C, indicating the formation depth less than 1 km. Type I cupriferous fluids in stage III vein have the homogenization temperatures and salinity of 168° to 365°C and 1.1 to 9.0 wt.% NaCl equiv. These fluid inclusions in stage III veins were trapped in quartz veins containing highly fractured breccia, indicating the predominance of boiling evidence. This corresponds to hydrostatic pressure of 50 to 80 bars. The $\delta^{34}S$ value of sulfide minerals increase slightly with paragenetic time and yield calculated $\delta^{34}S_{H2S}$ values of 0.8 to 3.7‰. There is no mineralogical evidence that fugacity of oxygen decreased, and it is thought that the oxygen fugacity of the mineralizing fluids have been buffered through reaction with magnetite. We interpreted the range of the calculated $\delta^{34}S_{H2S}$ values for sulfides to represent the incorporation of sulfur from two sources into the Xiaoxinancha Cu-Au hydrothermal fluids: (1) an isotopically light source with a $\delta^{34}S$ value of 1 to 2‰, probably a Mesozoic granitoid related to the ore mineralization. We can infer from the fact that diorite as the host rock in the Xiaoxinancha Cu-Au deposit area intruded plagiogranite; (2) an isotopically heavier source with a $\delta^{34}S$ value of > 4.0‰, probably the local porphyry.

Key words : alteration, ore mineralization, porphyry copper, fluid inclusion, sulfur isotope

1. INTRODUCTION

Although porphyry copper deposits have been intensively studied in the Mesozoic-Cenozoic belts of the China, their genesis is not relatively well understood. In China, the class of porphyry copper deposits is responsible for about a half of the total copper reserves. Especially, all known porphyry copper mineralization in China occurs in the Sino-Korean belts. These belts have not been completely stable since their consolidation in the Proterozoic, and for this reason many authors prefer the term paraplatform (Yang *et al.*, 1986; Ren *et al.*, 1987).

There have been few investigations on the style of the porphyry copper mineralization in the Jilin Province within the Sino-Korean belts up to date. The Xiaoxinancha Cu-Au deposit, located in NNE 800km of Beijing, is the only one of those being mined in the Jilin Province (Fig. 1) and have the average grade of 0.86% Cu, 3.81 g/t Au and 16.8 g/t Ag. On the basis of geologic setting and alteration patterens, it is thought that the overall mineralization characteristics of the Xiaoxinancha Cu-

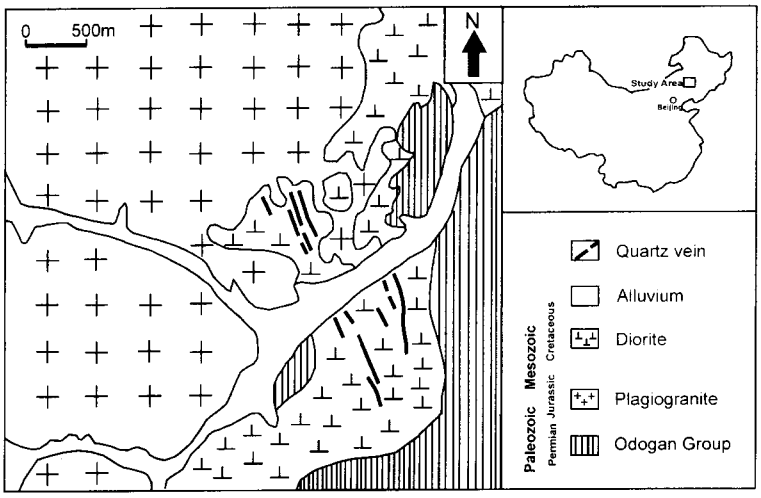

Fig. 1. Geological map of the Xiaoxinancha Cu-Au deposit, Yianbin, China.

Au deposit are very similar to those predicted by the generalized porpyry copper deposit model of Lowell and Guilbert (1970).

The purpose of this paper is to elucidate the hydrothermal history of the Xiaoxinancha Cu-Au deposit and idenfify the factors controlling Cu±Au ±Mo mineralization. Therefore, we conducted the following tasks: 1) identification of alteration and vein mineral paragenesis, 2) fluid inclusion and sulfur isotope studies for selected minerals.

2. GEOLOGIC SETTING

The Xiaoxinancha Cu-Au deposit in the Jilin province, located in NNE 800 km of Beijing, is hosted by diorite (Fig. 1). This diorite (70 to 110 Ma) is locally intruded by Yanshanian ganite and Late Cretaceous granite. It is composed of biotite, K-feldspar, hornblende and quartz with disseminated pyrite, and shows the characteristics of plotting within calc-alkaline field.

Odogan group (380 Ma) occupy the eastern part in this mining area and is composed of plagio-hornblende schist, biotite schist and mica schist. Accessory minerals consist of hornblende, biotite, quartz and K-feldspar with disseminated pyrite and chalcopyrite.

Plagiogranite (185 Ma) mostly occupy the western part adjacent the Odogan group and are composed of muscovite, K-feldspar, sericite and quartz with disseminated chalcopyrite and pyrite.

3. ORE VEINS AND ALTERATION

The Xiaoxinancha Cu-Au deposit shows a stockwork occurrence that is concentrated on the potassic and phyllic zones. Veins are mainly classified into two categories. Their strike and dips are as follows: 1) 10°~35° NW and 70°~80° SW, 2) 10°~50°W and 50°~74° NE. The Xiaoxinancha Cu-Au deposit in the south is being mined and reserves grading 0.8% Cu, 3.64 g/t Au and 16.8 g/t Ag and that in the north, 0.63% Cu, 3.80 g/t Au and 6.8 g/t Ag. The alteration is interpreted to represent a supergene blanket over deposit. Hydrothermal alteration at the Xiaoxinancha Cu-Au deposit is centered on the stock and was corresponded to the emplacement of stock. Early hydrothermal alteration was dominantly potassic and

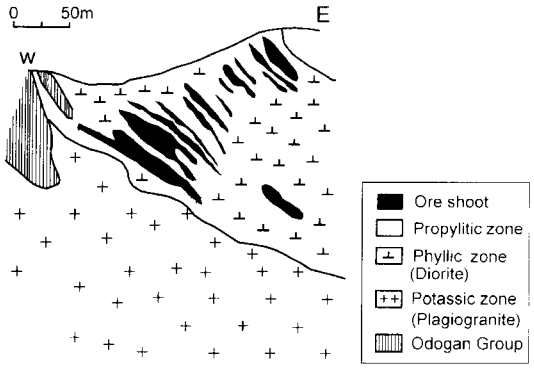

Fig. 2. Geologic section showing distribution of ore bodies overlapped with alteration zoning in the Xiaoxinancha Cu-Au deposit.

was followed by propylitic alteration (Fig. 2).

Potassic alteration is represented by the occurrence of actinolite and Mg-rich biotite, and is developed on plagiogranite in the top and central part of the deposit. This alteration displays a close spatial association with mineralization and is characterized by K-feldspar, actinolite, and Mg-rich biotite with disseminated pyrite. Phyllic alteration with increase in amount of muscovite is characterized by the replacement of almost all rock-forming silicates by sericite and quartz. It occurs as ore vein and upper-lower portion of diorite. Minor minerals associated with phyllic alteration are pyrite, chalcopyrite, native gold and electrum. Propylitic alteration is distributed into separate diorite and represented mainly by chloritization of primary and secondary biotite. Minor minerals associated with propylitic alteration are epidote, chlorite, calcite, pyrite and chalcopyrite. Carbonatization occurs as the latest veins and is distributed adjacent to diorite.

4. MINERAL PARAGENESIS

In the Xiaoxinancha Cu-Au deposit, chalcocite, often associated with hematite, accounts for the ore-grade copper, while chalcopyrite, bornite, quartz, epidote, chlorite and calcite constitute the typical gangue assemblages. Other minor opaque phases recognized in this study include pyrite, marcasite, native gold, electrum, hessite, hedleyite, volynskite, galenobismutite, covellite and goethite. Four stages of mineralization are defined and the brief

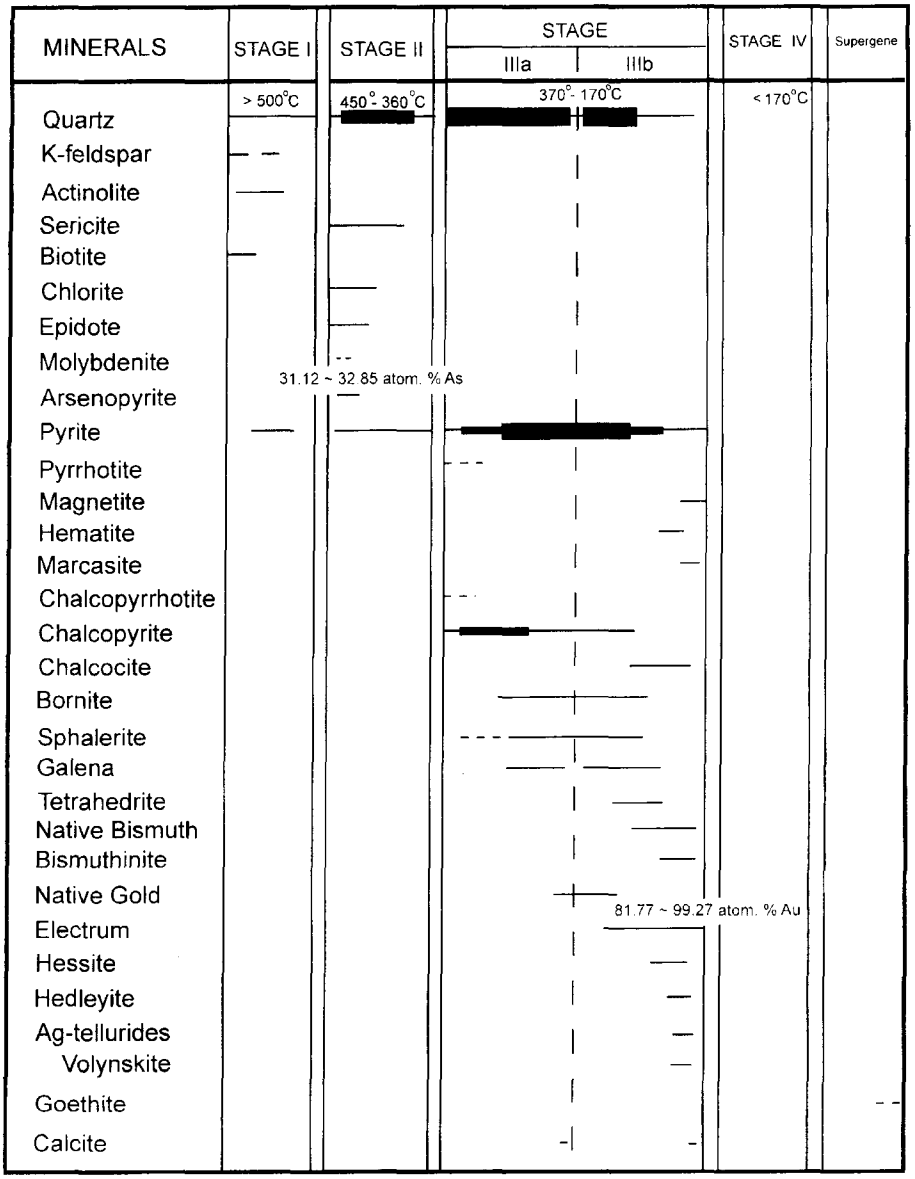

Fig. 3. Paragenetic sequence of the Xiaoxinancha Cu-Au deposit.

descriptions are as follows (Fig. 3).

Stage II mineralization is accompanied by a change from dominantly sericitic to propylitic (chlorite and epidote) alteration, but quartz persists as the principal gangue mineral in the veins. The vein quartz displays a variety of habits which range from fine-grained crustifications to coarse cavity fillings. It may suggests rapid changes in the physicochemical conditions of the ore fluid into open space supersaturated with solution. The sulfide mineral have the characteristics of primary precipitation and dendritic habit. And small amounts of pyrite+arsenopyrite+chalcopyrite with fine-grained quartz showing sericitic and silicic alteration occur. Arsenopyrite (31.12 to 32.85 atom.% As) occurs as euhedral grain throughout the veins which is commonly associated with pyrite and/or replaced partially pyrite and sphalerite.

Stage III mineralization is divided into two substages. Stage IIIa is characterized by the occurrence of pyrite-rich chalcopyrite and stage IIIb is characterized by the occurrence of base-metal+Bi-Te-Ag sulfosalts+chalcocite+hematite. Within the main fissure veins of stage IIIa mineralization, pyrrhotite+chalcopyrite assemblage were seen in various modes of replacement by bornite, chalcocite and hematite. Sphalerite is widespread throughout stage III veins. Fine- to medium-grained sphalerite is rarely impregnated into the silicified wall rock adjacent to the vein margins and dispersed as euhedral to subhedral grains. Sphalerite usually occurs as anhedral masses throughout the veins and is closely intergrown with pyrrhotite, chalcopyrite and galena. Bornite was rarely found on its own but occurred mostly as intermediate alteration phase of chalcopyrite. It may represent impurities within original chalcopyrite. Stage IIIb mineralization is composed of base-metal sulfides and precious metal bearing Bi-Te-Ag sulfosalts such as hessite, hedleyite and volynskite. Chalcocite is associated with late quatz, galena, chalcopyrite, electrum and Bi-Te-Ag sulfosalts. It was never seen to crosscut or replaced by chalcopyrite or bornite, although supergene alteration to covellite was occasionally observed. Coarse-grained tetrahedrite was similarly found as inclusions replacing chalcocite. Electrum (81.77 to 99.27 atom. % Au) occurs as small grains with galena, chalcopyrite, sphalerite and tetrahedrite. Hessite, hedleyite and volynskite occur with electrum within galena. Pyrite, or its polymorph marcasite, was frequently found as corroded relict grains in later bornite+hematite and chalcocite+hematite assemblages, implying the replacement of early Cu-Fe sulfide phases by copper-rich minerals.

Calcite frequently occurs as late vug-filling and/or in late crosscutting veins of pure carboantes in stage IV mineralization.

5. FLUID INCLUSION STUDIES

About fifty vein quartz samples for fluid inclusion study were collected from underground ore stopes and the surface area. Additional calcite samples were obtained from the post-ore carbonate vein. Sphalerite were not suitable to study the fluid inclusion study because of their opacity. Data were obtained on a FLUID Inc. gas flow heating-freezing stage calibrated with pure CO_2, H_2O synthetic inclusions and various kinds of organic solvents (Hollister and Burruss, 1976). Heating rates were varied widely but were maintained near 1°C/min for determination of melting temperatures and carbonaceous phase homogenization temperatures, and about 10°C/min for determination of total homogenization temperatures. On the measurements of melting points, repeated cycling techniques were used over the expected temperatures. Temperatures of total homogenization, and of melting (of carbonaceous phases, ice and clathrate) and carbonaceous phase homogenization have standard errors of ±1.0°C and ±0.2°C, respectively. In addition to microthermometric measurements, the mole fraction of each phase was visually determined on selected inclusions.

5.1. Compositional types of fluid inclusion

Fluid inclusions are abundant in quartz of all the vein types and most of inclusions examined during this study are 5 to 35 μm in diameter. Most of our measurements were conducted on fluid inclusions in stage II, III and IV veins. Fluid inclusions were classified into three main types based on the proportion of phases at room temperatures (25°C).

Liquid-rich aqueous inclusions (type I) are the predominant inclusion type. These fluid inclusions are common in all mineralized quartz veins and barren calcite veins. The diameters range from 5 to 10 μm. The proportion of vapor bubbles is variable but less than 30% in volume. And, it is impossible to establish a consistent fluid inclusion chronology because repeated fracturing and healing both during and after quartz deposition frequently prevent distinguishing among primary and secondary inclusions using normal criteria (Roedder, 1984).

Type II inclusions occur as vapor-rich and variable in size (15 to 40 μm). They have a gas bubble of more than 40 vol.% (mostly>50%) at room temperature. They are usually irregular in shape and occasionally show the necking-down phenomena. They occur as small amounts along the planes crosscutting quartz grains, suggesting their primary origin. They do not contain CO_2 and are interpreted to be simple H_2O-salt inclusion.

Type III inclusions consist of liquid + vapor +

halite + other daughter minerals at room temperatures. These fluid inclusions were subdivided into three types, based on the presence or absence of sylvite on their homogenization behavior. Type IIIa inclusions contain halite + H_2O and homogenize by halite dissolution at temperatures greater than liquid-vapor homogenization. Type IIIb inclusions homogenize to liquid by vapor disappearance after halite dissolution. Type IIIc inclusions contain sylvite in addition to halite + other daughter minerals. Commonly, five to seven daughter minerals are present in the type IIIc inclusions. Both halite and sylvite occur as large, sharp to slightly rounded crystals. This inherent difficulty of clarity has shown in crack-healing experiments with quartz (Shelton and Orville, 1980; Bodnar, 1983).

5.2. Heating and freezing data

620 fluid inclusions (540 primary and 80 secondary inclusions) were examined in the Xiaoxinancha Cu-Au deposit. Salinity data were reported based on freezing point depression in the system H_2O-NaCl for H_2O-rich type (Bodnar, 1993) and H_2O-NaCl-KCl type (Roedder, 1984).

Fluid inclusions in stage II vein: The first ice melting temperature of primary type I inclusions, although it was so difficult to observe that only a few measurements were recorded, was recognized at near -21°C. Final ice melting temperatures in the primary type I inclusions range -0.9° to -10.8°C, corresponding to the salinities of 1.6 to 14.8 wt.% eq. NaCl. Those in secondary type I inclusions are -0.2° to -1.1°C, corresponding to the salinities of 0.4 to 1.9 wt.% eq. NaCl (Fig. 4). Primary and secondary type I inclusions homogenized totally to liquid phase at temperatures of 272° to 545°C and 152° to 268°C, respectively (Fig. 5). Final ice melting temperatures of type II inclusions range -3.4° to -20.1°C, corresponding to the salinities of 5.6 to 22.1 wt.% NaCl. (Fig. 4). They homogenize totally to vapor phase at temperatures of 303° to 482°C (Fig. 5). T_{NaCl} of type IIIa and IIIb inclusions ranges 373° to 464°C and 177° to 218°C, corresponding to the salinities of 44.2 to 52.4 and 31.0 to 33.3 wt.% NaCl, respectively (Fig. 4). Total homogenization temperatures of type IIIa and IIIb inclusions, including useful decrepitation temperatures, were 304° to 360°C and 303° to 393°C, respectively (Fig. 5). The salinities and approx-

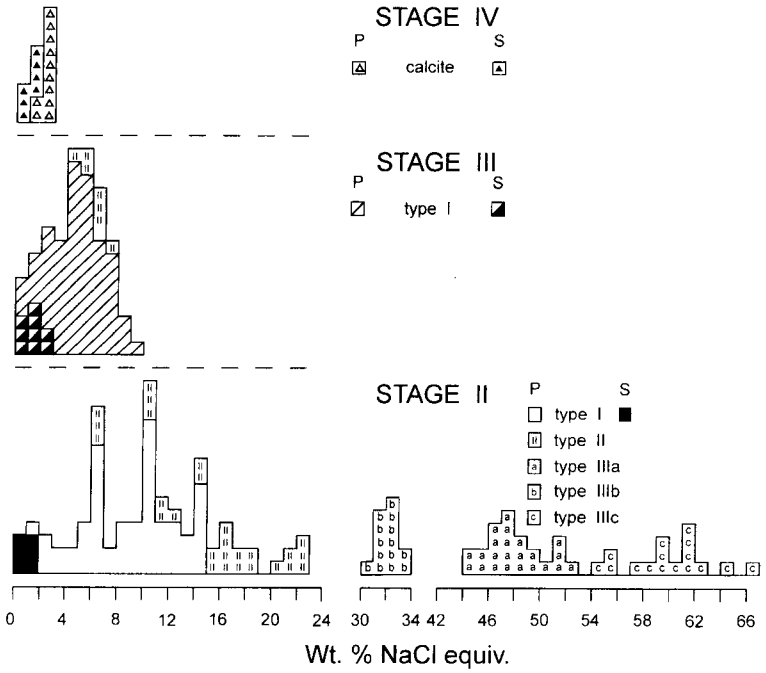

Fig. 4. Salinities of fluid inclusions from the Xiaoxinancha Cu-Au deposit.

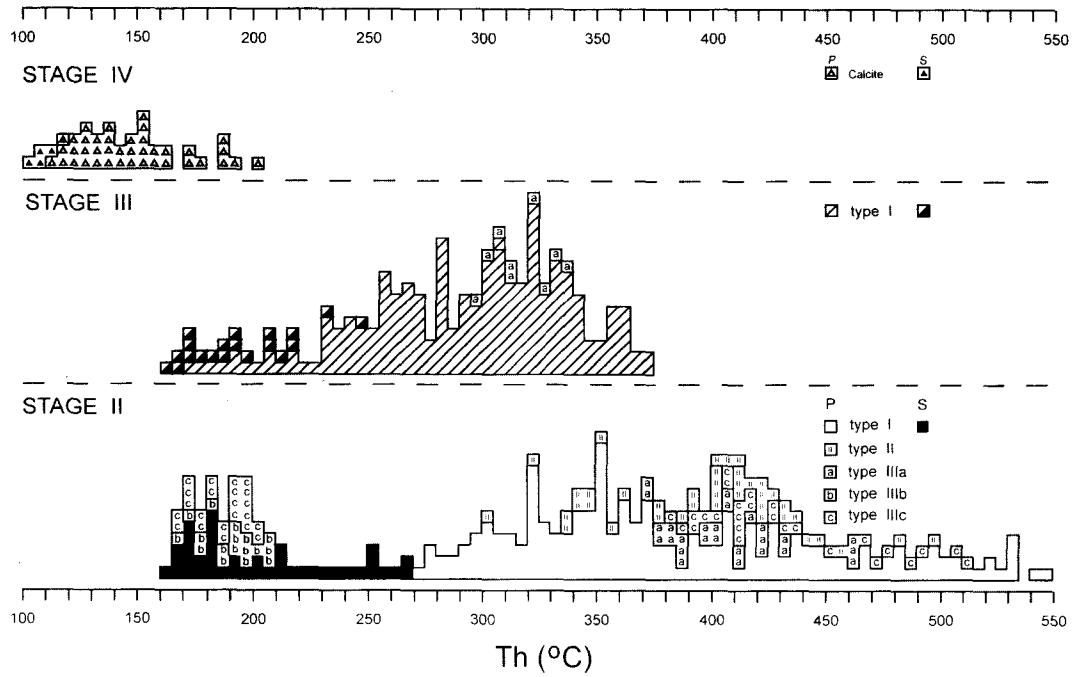

Fig. 5. Homogenization temperatures of fluid inclusions from the Xiaoxinancha Cu-Au deposit.

imate bulk compositions of type IIIc inclusions were estimated by measuring the dissolution temperature of halite (383° to 495°C) and sylvite (178° to 212°C) using NaCl-KCl-H_2O phase diagram, resulting in total estimated NaCl+KCl contents of 54.3 to 66.9 wt.% (Fig. 4). Calculated K/Na atomic ratios for type IIIc inclusion range from 0.35 to 0.42. Bulk compositions of the type IIIc inclusions estimated using halite and sylvite dissolution temperatures ignore the effects of $CaCl_2$, $FeCl_2$ and other species on th solubility of NaCl and KCl.

Fluid inclusions in stage III vein: Final ice melting temperatures of primary type I inclusion range from -0.6° to -5.8°C, corresponding to the salinities of 1.1 to 9.0 wt.% NaCl equiv. (Fig. 4). Total homogenization temperatures of primary type I inclusion range from 168° to 365°C (Fig. 5). It was not suitable for seconadary type I inclusions to obtain salinity data in freezing experiments because of their small size (5 to 8 μm). Nonetheless, the obtained result of salinity data and total homogenization temperatures of secondary type I inclusion are 0.4 to 2.7 wt.% equiv. NaCl and 168° to 247°C (Fig. 4 and 5). Final ice melting temperatures of type II inclusion range from -3.2° to -4.5°C, corresponding to the salinities of 4.8 to 7.2 wt.% NaCl equiv. (Fig. 4). Small amounts of type II inclusions coexisting type I inclusions homogenized at 295° to 338°C (Fig. 5).

Fluid inclusions in stage IV vein: The salinity data of primary type I fluid inclusions in white calcite are 1.2 to 2.9 wt.% NaCl (Fig. 4) and their homogenization temperature range from 112° to 204°C (Fig. 5). Final ice melting temperatures of secondary type I inclusion range from -0.1° to -1.0°C, corresponding to the salinities of 0.2 to 1.7 wt.% NaCl equiv. (Fig. 4). They homogenized at 103° to 118°C (Fig. 5).

5.3. Pressure considerations

The evolution history of mineralizing fluid observed at Xiaoxinancha Cu-Au deposit, Jilin province, are as follows. In stage II vein, early boiling occurred at 497°C was succeeded by the occurrence of halite-bearing type III fluid inclusion with homogenization temperature as much as 100°C lower. The salinities of type III fluid inclusion in stage II vein are 54.3 to 66.9 wt.% NaCl equiv. NaCl+KCl at 383° to 495°C (Fig. 4 and 5).

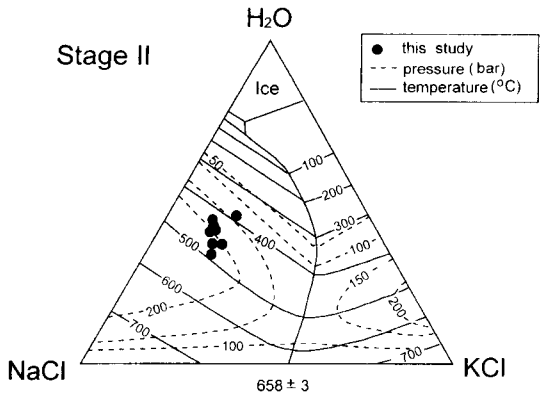

Fig. 6. NaCl-KCl-H_2O phase diagram showing the composition of fluid inclusions determined of halite and sylvite (phase diagram after Roedder, 1984).

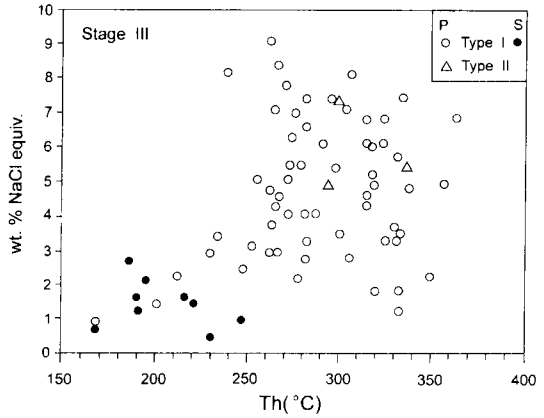

Fig. 7. Homogenization temperature versus salinities of fluid inclusions from the Xiaoxinancha Cu-Au deposit.

Considering this result, the present surface of the stock hosting the Xiaoxinancha Cu-Au deposit may appear at depth less than 1 km (Chou, 1987; Bodnar, 1992, Fig. 6).

Type I cupriferous fluids in stage III vein have the homogenization temperatures and salinity of 168° to 365°C and 0.4 to 9.0 wt.% NaCl equiv. (Fig. 7). These fluid inclusions in stage III veins were trapped in quartz veins containing highly fractured breccia, indicating the predominance of boiling evidence. Depths corresponding to hydrostatic pressure of 50 to 80 bars are inferred 190 to 300 m (Haas, 1971).

Conclusively, formation of this porphyry copper deposit is thought to be a result of cooling followed by mixing with dilute and cooler meteoric water with time.

Table 1. Sulfur isotope data of sulfide minerals from the Xiaoxinancha Cu-Au deposits in the Jilin Province, Republic of the China.

Stage	Sample no.	Mineral	$\delta^{34}S$ (‰)	T (°C)	$\delta^{34}S_{H2S}$ (‰)[1)]
II	S-1-5-1	chalcopyrite	2.6	450	2.7
	S-1-5-2	pyrite	3.6	450	0.8
	S-2	pyrite	3.1	370	2.1
	S-4	pyrite	2.8	370	1.8
	S-6	chalcopyrite	2.3	360	2.4
III	S-7-1	pyrrhotite	1.9	330	1.6
	S-7-2	chalcopyrite	2.6	330	2.7
	S-10-1	chalcopyrite	3.2	350	3.3
	S-10-2	pyrrhotite	1.5	350	1.3
	S-11-1	chalcopyrite	2.3	350	2.4
	S-11-2	chalcopyrite	2.4	350	2.5
	S-11-3	pyrrhotite	1.9	350	1.6
	S-12-1	chalcopyrite	3.6	330	3.7
	S-12-2	pyrrhotite	2.1	330	1.8
	S-20	pyrite	3.2	300	2.0
	S-27	pyrrhotite	2.0	310	1.7
	S-28	pyrite	3.4	310	2.2
	S-31-1	pyrrhotite	2.3	320	2.0
	S-31-2	chalcopyrite	2.8	320	1.9
	S-34	chalcopyrite	2.9	280	3.1
	S-39	pyrite	3.1	270	1.7
	S-46	chalcopyrite	3.0	270	3.2
	S-47	chalcopyrite	2.9	280	3.1

[1)]Based on fluid inclusion and/or sulfur isotope temperatures and paragenetic constraints.

5.4. Sulfur isotope study

In this study, we measured sulfur isotope compositions of sulfides. Standard technique for extraction and analysis was used by Grinenko (1962). Isotope data are reported in standard δ notation relative to the Canyon Diablo Troilite (CDT) standard for sulfur. The standard error of each analysis is approximately ±0.1‰ for S (Table 1).

Analyses of sulfur isotope in the Xiaoxinancha Cu-Au deposit were performed on twenty-three monomineralic samples from stage II and III veins. The minerals measured have the following $\delta^{34}S$ values: stage II, chalcopyrite, 2.3 to 2.6‰, pyrite, 2.8 to 3.6‰; stage III, chalcopyrite, 2.3 to 3.6‰, pyrite, 3.1 to 3.4‰, pyrrhotite, 1.5 to 2.3‰ (Table 1). The presence of pyrrhotite+pyrite+magnetite and the alteration assemblage of musco-

vite+quartz may indicate that sulfur in the fluid was dominantly H_2S. Assuming the depositional temperatures of 360° to 450°C for stage II sulfides and 270° to 350°C for stage III sulfides and using the compiled data of Ohmoto and Rye (1979), the calculated $\delta^{34}S_{H2S}$ values are as follows: stage II, chalcopyrite, 2.4 to 2.7‰, pyrite, 0.8 to 2.1‰; stgae III, chalcopyrite, 1.9 to 3.7‰, pyrite, 1.7 to 2.2‰, pyrrhotite, 1.3 to 2.0‰ (Table 1). The calculated $\delta^{34}S_{H2S}$ value for the chalcopyrite as mineralic bands at the vein margin is higher than those for other sulfides. Two possible explanations for this phenomenon are (1) an isotopic disequilibrium with ore fluids and (2) a greater contribution of heavier sulfur. The $\delta^{34}S_{H2S}$ values indicate a slight increase of 0.8 to 3.7‰ with paragenetic time. There is no mineralogical evidence that fugacity of oxygen decreased, and the oxygen fugacity of the mineralizing fluids could have been buffered through reaction with magnetite (Kwak *et al.*, 1986). We prefer to interpret the range of the calculated $\delta^{34}S_{H2S}$ values for sulfides to represent the incorporation of sulfur from two sources into the Xiaoxinancha Cu-Au hydrothermal fluids: (1) an isotopically light source with a $\delta^{34}S$ value of 1 to 2, probably a Mesozoic granitoid related to the ore mineralization. We can infer from the fact that diorite as the host rock in the Xiaoxinancha Cu-Au deposit area intruded plagiogranite; (2) an isotopically heavier source with a $\delta^{34}S$ value of >4.0‰, probably the local porphyry. The predominance of H_2S in the fluids may indicate that the range of the $\delta^{34}S_{H2S}$ values of 0.8 to 3.7‰ is a good approximation of the $\delta^{34}S_{\Sigma S}$ value of the ore fluid.

6. SUMMARY

1. The Xiaoxinancha Cu-Au deposit in the Jilin province, located in NNE 800 km of Beijing, is hosted by diorite. The ore mineralization of Xiaoxinancha Cu-Au deposit show a stockwork occurrence that is concentrated on the potassic and phyllic zones. The Xiaoxinancha Cu-Au deposit reserves grading 0.63 to 0.8% Cu, 3.64 to 3.80 g/t Au and 6.8 to 16.8 g/t Ag.

2. The alteration occurrence of Xiaoxinancha Cu-Au deposit is interpreted to represent a supergene blanket over deposit. Hydrothermal alteration at the Xiaoxinancha Cu-Au deposit is centered on the stock and was broadly corresponded to the emplacement of stock. Early hydrothermal alteration was dominantly potassic and was followed by propylitic alteration.

3. In the Xiaoxinancha Cu-Au deposit, chalcocite, often associated with hematite, account for the ore-grade copper, while chalcopyrite, bornite, quartz, epidote, chlorite and calcite constitute the typical gangue assemblage. Other minor opaque phases recognized in this study include pyrite, marcasite, native gold, electrum, hessite, hedleyite, volynskite, galenobismutite, covellite and goethite.

4. Fluid inclusion data indicate that the formation of this porphyry copper deposit is thought to be a result of cooling followed by mixing with dilute and cooler meteoric water with time. In stage II vein, early boiling occurred at 497°C was succeeded by the occurrence of halite-bearing type III fluid inclusion with homogenization temperature as much as 100°C lower. The salinities of type III fluid inclusion in stage II vein are 54.3 to 66.9 wt.% NaCl equiv. NaCl + KCl at 383° to 495°C, indicating the formation depth less than 1km. Cupriferous fluids in stage III vein have the homogenization temperatures and salinity of 168° to 365°C and 1.1 to 9.0 wt.% NaCl equiv. These fluid inclusions in stage III veins were trapped in quartz veins containing highly fractured breccia, indicating the predominance of boiling evidence. This corresponds to hydrostatic pressure of 50 to 80 bars.

5. The $\delta^{34}S$ value of sulfide minerals increase with paragenetic time and yield calculated $\delta^{34}S_{H2S}$ values of 0.8 to 3.7‰. We interpreted the range of the calculated $\delta^{34}S_{H2S}$ values for sulfides to represent the incorporation of sulfur from two sources into the Xiaoxinancha Cu-Au hydrothermal fluids: (1) an isotopically light source with a $\delta^{34}S$ value of 1 to 2‰, probably a Mesozoic granitoid related to the ore mineralization. We can infer from the fact that diorite as the host rock in the Xiaoxinancha Cu-Au deposit area intruded plagio granite; (2) an isotopically heavier source with a $\delta^{34}S$ value of > 4.0, probably the local porphyry.

ACKNOWLEDGEMENTS

This research was financially supported by Korea University Grant (to Prof. So) and partially by the

Center for Mineral Resources Research, Korea University.

REFERENCES

Bodnar, R.J. (1983) A method of calculating fluid-inclusion volume based on vapor bubble diameters and P-V-T-X properties of inclusion fluids. Economic Geology, v. 78, p. 535-542.

Bodnar, R.J. (1992) Experimental determination of the liquids and isochores of a 40 wt.% NaCl-H_2O solution using synthetic fluid inclusions [abs]. Pan-American Conference on Research in Fluid Inclusions(PACROFI IV), 4th, Lake Arrowhead, CA, May 22-25, 1992, Program and Abstracts, v. 4, p.14.

Bodnar, R.J. (1993) Revised equation and table for determining the freezing point depression of H_2O-NaCl solutions. Geochimica et Cosmochimica Acta, v. 57, p. 683-684.

Chou, I.M. (1987) Phase relation in the system NaCl-KCl-H_2O. III: Solubilities of halite in vapor-saturated liquids above 445 and redetermination of phase equilibrium properties in the system NaCl-H_2O to 1000 and 1500 bars. Geochimica et Cosmochimica Acta, v. 51, p. 1965-1975.

Grinenko, V.A. (1962) Preparation of sulfur dioxide for isotopic analysis. Zeitschr. Neorganische Chemie, v. 7, p. 2478-2483.

Haas, J.L. Jr. (1971) The effect of salinity on the maximum thermal gradient of a hydrothermal system at hydrostatic pressure. Economic Geology, v. 66, p. 733-742.

Hollister, L.S. and Burruss, R.C. (1976) Phase equilibria in fluid inclusions from the Khtada Lake metamorphic complex. Geochim. Comochim. Acta., v. 40, p. 163-175.

Kwak, T.A.P., Brown, W.M., Abeysinghe, P.B. and Tan, T.H. (1986) Fe solubilities in very saline hydrothermal fluids. Their relation to zoning in some ore deposits. Economic Geology, v. 81, p. 447-465.

Lowell, J.D. and Guilbert, J.D. (1970) Lateral and vertical alteration mineralization in porphyry ore deposit. Economic Geology, v. 65, p. 373-408.

Ohmoto, H. and Rye, R.O. (1979) Isotopes of sulfur and carbon, in Barnes, H.L.,ed., Geochemistry of hydrothermal ore deposits. New York, Wiley Interscience, p. 509-567.

Ren, J.S., Jiang, C.F., Zhang, Z.K. and Qin, D.Y. (1987) Geotectonic evolution of China, Beijing.

Roedder, E. (1984) Fluid inclusions. Reviews in Mineralogy, v. 12, 644p.

Shelton, K.L. and Orville, P.M. (1980) Formation of synthetic fluid inclusions in batural quartz. American Mineralogist, v. 65, p. 1233-1236.

Yang, Z.Y., Cheng, Y.C. and Wang, H.Z. (1986) The geology of China, Oxford Monograph on Geology and Geophysics no. 3. Oxford Univ. Press, Oxford.

2002년 4월 6일 원고접수, 2002년 6월 14일 게재승인.